African Review of Economics and Finance (Online), **18**, 1–27
ISSN (Print) 2042-1478
ISSN (Online) 2410-4906

ARTICLE

The changing hierarchy of G7 equity spillovers to South Africa: Evidence across time and investment horizons

Jakubose Sibanda[1] and Jones Odei-Mensah[*,2]

[1]TSIBA Business School, Cape Town, South Africa
[2]Wits Business School, Faculty of Commerce, Law and Management, University of the Witwatersrand, Johannesburg, South Africa
[*] Corresponding Author: jones.odei-mensah@wits.ac.za

Abstract

This study examines whether the hierarchy of G7 connectedness with the South African equity market remains stable through time and across investment horizons. Using 4,520 daily USD-denominated stock-index returns for South Africa and the seven G7 markets from 3 July 2006 to 27 October 2023, the study combines a Time-Varying Parameter Vector Autoregressive (TVP-VAR) connectedness framework with bivariate and multivariate wavelet analysis. The ordinary Total Connectedness Index (TCI) is 73.06%, while the corrected TCI is 83.49%, indicating substantial cross-market dependence, and the JSE is predominantly a net receiver within the estimated network. On average, the largest contributions to JSE forecast-error variance originate from the United Kingdom, France and Germany, whereas U.S.–JSE bilateral connectedness rises sharply around the COVID-19 episode, reaching its highest observed level just below 80%. Bivariate wavelet evidence further shows that JSE–G7 co-movement and lead–lag relationships vary across time and investment horizons. In the multivariate analysis, the CAC40 maximizes wavelet multiple correlation at all seven MODWT detail levels. Wavelet multiple cross-correlation similarly identifies the CAC40 as the maximizing market at every scale, with predominantly contemporaneous maxima and a one-day lead at the 64–128-day horizon. The findings show that system-wide connectedness, JSE-specific exposure, episode-specific bilateral connectedness and horizon-specific multivariate dependence need not identify the same G7 market as most important for South Africa.

Keywords: South African Equity Market, G7 Stock Markets, Equity Spillovers, Dynamic Connectedness, Directional Connectedness, Investment Horizons

JEL classification: G15, F36, C58

Article history: Received: February 9, 2025 || Accepted: September 8, 2026

1. Introduction

Global equity markets are increasingly interconnected, allowing shocks to propagate rapidly across borders. In 2023, global equity trading exceeded USD 130 trillion, illustrating the scale of cross-border financial exposure (Statista, 2024). This vulnerability became particularly visible during COVID-19, when global equities lost nearly USD 6 trillion within a single week in February 2020 (Hasan et al., 2021). The pandemic also produced sharp increases in co-movement and volatility across G7 equity markets (Izzeldin et al., 2021; Rehman et al., 2021). Developing markets proved particularly sensitive, experiencing stronger pandemic-related effects than during the Global Financial Crisis (Tabash et al., 2024). These episodes demonstrate that financial integration can rapidly transform external disturbances into systemic market risks. Understanding the direction, intensity, and persistence of cross-border shock transmission therefore remains central to diversification, risk management, and financial stability.

South Africa provides a distinctive setting for examining external equity-market transmission. The Johannesburg Stock Exchange (JSE) is Africa's most developed and internationally integrated equity market, with market capitalisation exceeding USD 1 trillion (Agyei-Ampomah, 2011; Mensah and Alagidede, 2017). Yet its importance extends beyond market size. Nyakurukwa and Seetharam (2022) identify South Africa as the most influential African equity market, transmitting the largest share of information across the regional network. Recent multiscale evidence similarly shows that South Africa can assume a leading role among African markets at particular investment horizons (Junior et al., 2024). At the same time, the JSE remains unusually exposed to global financial conditions, with connectedness to international markets rising markedly during global disturbances such as COVID-19 (Lawrence et al., 2024b). South Africa therefore occupies an unusual position: it is regionally influential within Africa, yet highly exposed to shocks originating in advanced markets.

South Africa's international integration does not, however, reveal the structure of its external exposure. Aggregate connectedness can remain high even when the relative importance of individual foreign markets changes substantially. Moreover, the market that dominates the wider international network need not be the market exerting the strongest direct influence on the JSE, while crisis-specific and horizon-specific leadership may differ again. This distinction matters because the origin and persistence of external shocks shape both diversification opportunities and financial-stability risks. The central issue is therefore whether the hierarchy of G7 influence on the JSE is stable or whether different markets emerge as dominant sources of South African equity shocks across time and investment horizons.

Two complementary theoretical perspectives suggest that the hierarchy of external market influence need not remain stable. The interdependence and contagion literature argues that shocks propagate across national equity markets through trade, portfolio rebalancing, liquidity, and information channels, with these transmission mechanisms becoming particularly important during periods of financial stress (Rigobon, 2019). Accordingly, both the intensity and the source of cross-market transmission may change through time. The Heterogeneous Market Hypothesis (HMH), in turn, recognises that market participants operate over different investment horizons and respond differently to information according to their trading objectives, risk preferences, and holding periods. Consequently, a market that exerts strong influence over the JSE at short horizons need not retain the same importance at medium or long horizons. Taken together, these perspectives imply that the hierarchy of G7 influence on South Africa may be both time-varying and horizon-dependent, providing the theoretical basis for examining whether external market leadership is invariant across these dimensions.

A separate literature examines connectedness within African equity markets and consistently identifies substantial cross-country heterogeneity. Although average intra-African integration is generally weak, South Africa frequently occupies a disproportionately influential position. Nyakurukwa and Seetharam (2022) using transfer entropy, find limited information flows among African exchanges but identify South Africa as the most influential market in the system. Yaya et al. (2024) further show that regional leadership is state-dependent, with South Africa assuming a dominant transmitting role under bearish market conditions. Multiscale evidence reaches a similar conclusion, with Junior et al. (2024) finding that lead-lag relationships among African markets vary across time and frequencies, with South Africa leading the regional system at selected medium-term horizons. Earlier evidence also shows that African markets are exposed to shocks originating in major developed markets, particularly during episodes of global stress. The African literature therefore establishes both

South Africa's regional importance and the conditional nature of market leadership, but provides less resolution on the relative composition of the JSE's exposure to individual advanced-market sources.

South Africa-specific studies further demonstrate that the JSE's external connectedness is economically significant but unstable. Bonga-Bonga and Phume (2022) document directional transmission between South African and Nigerian equities, while Gopane (2023) links stronger South Africa–BRIC economic integration to greater stock-market integration. Batondo and Uwilingiye (2022) show that South Africa's co-movement with the United States varies across investment horizons and crisis episodes using multiscale wavelet analysis. Lawrence et al. (2024b), using a TVP-VAR framework, provides direct evidence that South Africa's global connectedness changes across distinct shocks, for instance, international connectedness rises during COVID-19 but weakens during the domestic load-shedding crisis. Collectively, these studies establish that South Africa's external exposure varies across markets, episodes, and horizons. However, they typically employ regional or BRICS comparison groups, selected advanced-market benchmarks, or aggregate global indices. Consequently, they do not fully resolve whether the relative importance of the complete set of individual G7 markets facing the JSE remains stable.

Methodologically, the literature has also progressed beyond static measures of integration. TVP-VAR connectedness models establish that directional spillovers evolve continuously through calendar time, while wavelet-based approaches show that co-movement and lead-lag relationships differ across investment horizons. Multiscale techniques have already been applied to African equities, BRICS–US relations, and G7 markets, while TVP-VAR models have been used in both G7-BRICS and South African settings. These approaches therefore provide established tools for studying different dimensions of financial dependence. The unresolved issue is not the availability of techniques for detecting time variation or horizon dependence, but whether these dimensions produce different conclusions about the relative G7 markets that matter for South Africa.

Taken together, the literature establishes three important facts: G7 markets are major sources of shocks to emerging equities; South Africa is unusually internationally connected relative to many African markets; and both connectedness and market leadership can vary through time and across investment horizons. What remains comparatively underexplored is whether the *relative hierarchy* of individual G7 influence on the JSE itself is stable across these dimensions. Existing network-wide studies can identify dominant transmitters within the broader G7-BRICS system without establishing whether the same markets dominate South Africa directly, while bilateral and selected-benchmark studies cannot recover the complete G7 hierarchy facing the JSE. This distinction matters because aggregate connectedness may remain elevated even as the principal source of South African external risk changes. The central unresolved question is therefore: *Does the hierarchy of individual G7 influence on the JSE remain stable through time and across investment horizons, or do different G7 markets emerge as dominant sources of South African equity shocks?*

This study addresses this question by placing the JSE at the centre of a complete G7 equity network and examining whether the relative importance of individual G7 markets changes across calendar time and investment horizons. The analysis uses daily equity returns for South Africa and all seven G7 markets from July 2006 to October 2023. TVP-VAR connectedness measures identify evolving directional and bilateral shock transmission, while wavelet coherence and phase differences reveal horizon-specific co-movement and leadership. Wavelet multiple correlation and cross-correlation provide complementary evidence on multivariate dependence and longer-horizon leadership. The purpose of combining these approaches is therefore not methodological novelty, but to determine whether alternative dimensions of connectedness reveal the same or different external hierarchy for South Africa.

Motivated by this unresolved question, this study examines the changing hierarchy of G7 influence on the South African equity market. Specifically, it investigates whether the relative importance of individual G7 markets to the JSE remains stable through calendar time and across investment horizons.

Using daily equity returns for South Africa and all seven G7 markets from July 2006 to October 2023, the analysis employs complementary empirical approaches. A TVP-VAR connectedness framework identifies evolving directional and bilateral shock transmission and its intensification around major crisis episodes. Cross-wavelet coherence and phase differences are then used to examine whether bilateral JSE–G7 relationships and lead–lag patterns vary across investment horizons, while wavelet multiple correlation and wavelet multiple cross-correlation provide complementary evidence on multivariate dependence and longer-horizon market leadership. Rather than treating these techniques as a source of methodological novelty, their combined use enables the central question to be examined from distinct temporal and horizon-specific dimensions.

The findings reveal that a changing rather than invariant hierarchy characterises South Africa's external G7 exposure when different dimensions of connectedness are considered. Although the JSE is predominantly a net receiver within a highly connected system, the most important depends on the dimension examined. On average, the largest contributions to JSE forecast-error variance originate from the United Kingdom, France and Germany, followed by Canada and Italy, whereas the United States assumes substantially greater bilateral importance during particular episodes, most notably around COVID-19. Bivariate wavelet evidence further shows that JSE-G7 co-movement and lead-lag relationships vary across time and investment horizons. In the multivariate wavelet analysis, however, the CAC40 consistently maximizes both wavelet multiple correlation and wavelet multiple cross-correlation across all seven detail levels, with the WMCC maximum occurring contemporaneously at most scales and at a one-day lead at the 64–128 day horizon.

Two contributions follow from these findings. First, the study shows that South Africa does not face a single permanently dominant G7 source of external equity connectedness when alternative dimensions of dependence are considered. Second, it demonstrates that system-wide connectedness, direct JSE forecast-error variance exposure, episode-specific bilateral connectedness and multivariate horizon-specific dependence need not identify the same market as most important. These findings imply that portfolio analysis and external-risk surveillance for South Africa should distinguish among individual source markets, episodes and investment horizons rather than relying solely on aggregate G7 connectedness measures.

The paper proceeds as follows: Section 2 presents the methodology, Section 3 describes the data, Section 4 reports and discusses the results, and Section 5 concludes with policy implications.

2. Methodology

This study adopts a combination of wavelet-based multi-scale analysis and a Time-Varying Parameter Vector Autoregressive (TVP-VAR) connectedness framework to examine stock market integration between South Africa and G7 markets. Wavelet methods are employed to decompose equity returns into short-, medium-, and long-term components, allowing connectedness to be analysed across different investment horizons.

2.1 TVP-VAR-based dynamic connectedness approach

The dynamic connectedness analysis is based on the Time-Varying Parameter Vector Autoregressive (TVP-VAR) framework. Following Antonakakis et al. (2020), and given that the Bayesian Information Criterion (BIC) selects one lag, the TVP-VAR(1) model is specified as

$$\mathbf{z}_t = \mathbf{B}_t\mathbf{z}_{t-1} + \mathbf{u}_t, \qquad \mathbf{u}_t \sim N(\mathbf{0}, \mathbf{S}_t), \tag{1}$$

where $\mathbf{z}_t$ is a $k \times 1$ vector of stock-market returns, $\mathbf{B}_t$ is a $k \times k$ matrix of time-varying autoregressive coefficients, and $\mathbf{S}_t$ is the $k \times k$ time-varying variance–covariance matrix of the innovations.

The time-varying coefficients evolve according to

$$\mathrm{vec}(\mathbf{B}_t) = \mathrm{vec}(\mathbf{B}_{t-1}) + \mathbf{v}_t, \qquad \mathbf{v}_t \sim N(\mathbf{0}, \mathbf{R}_t), \tag{2}$$

where $\mathbf{v}_t$ is a $k^2 \times 1$ vector of state innovations and $\mathbf{R}_t$ is its $k^2 \times k^2$ variance–covariance matrix.

To obtain the forecast-error variance decomposition required for the connectedness analysis, the TVP-VAR representation is transformed into its corresponding time-varying moving-average (TVP-VMA) representation:

$$\mathbf{z}_t = \sum_{h=0}^{\infty} \mathbf{A}_{h,t}\mathbf{u}_{t-h}, \qquad \mathbf{A}_{0,t} = \mathbf{I}_k, \tag{3}$$

where $\mathbf{A}_{h,t}$ denotes the $k \times k$ time-varying moving-average coefficient matrix associated with forecast horizon h. Throughout the analysis, t indexes calendar time, whereas h indexes the forecast horizon. The empirical connectedness measures are computed using a forecast horizon of $H = 20$ days.

Following Koop et al. (1996) and Pesaran and Shin (1998), the H-step-ahead generalized forecast-error variance decomposition (GFEVD) is defined as

$$\theta^{g}_{ij,t}(H) = \frac{\sigma^{-1}_{jj,t} \sum_{h=0}^{H-1} \left(\mathbf{e}_i'\mathbf{A}_{h,t}\mathbf{S}_t\mathbf{e}_j\right)^2}{\sum_{h=0}^{H-1} \left(\mathbf{e}_i'\mathbf{A}_{h,t}\mathbf{S}_t\mathbf{A}'_{h,t}\mathbf{e}_i\right)}, \tag{4}$$

where $\sigma_{jj,t}$ denotes the jth diagonal element of $\mathbf{S}_t$, while $\mathbf{e}_i$ and $\mathbf{e}_j$ are $k \times 1$ selection vectors containing unity in positions i and j, respectively, and zeros elsewhere. Thus, $\theta^{g}_{ij,t}(H)$ measures the proportion of the H-step-ahead forecast-error variance of market i attributable to shocks originating in market j. The generalized decomposition is invariant to variable ordering (Pesaran and Shin, 1998; Diebold and Yilmaz, 2012).

Because generalized variance shares do not necessarily sum to unity, they are normalised as

$$\tilde{\theta}^{g}_{ij,t}(H) = \frac{\theta^{g}_{ij,t}(H)}{\sum_{m=1}^{k} \theta^{g}_{im,t}(H)}, \tag{5}$$

such that

$$\sum_{j=1}^{k} \tilde{\theta}^{g}_{ij,t}(H) = 1. \tag{6}$$

Based on the normalised GFEVD, directional connectedness *from* all other markets to market i is defined as

$$FROM_{i,t} = 100 \sum_{\substack{j=1 \\ j\neq i}}^{k} \tilde{\theta}^{g}_{ij,t}(H), \tag{7}$$

while directional connectedness *to* all other markets from market i is

$$TO_{i,t} = 100 \sum_{\substack{j=1 \\ j\neq i}}^{k} \tilde{\theta}^{g}_{ji,t}(H). \tag{8}$$

Net total directional connectedness is consequently

$$NET_{i,t} = TO_{i,t} - FROM_{i,t}. \tag{9}$$

A positive value of $NET_{i,t}$ identifies market i as a net transmitter of shocks, whereas a negative value identifies it as a net receiver.

The conventional Total Connectedness Index (TCI) is given by

$$TCI_t = \frac{100}{k} \sum_{i=1}^{k} \sum_{\substack{j=1 \\ j \neq i}}^{k} \widetilde{\theta}^{g}_{ij,t}(H). \tag{10}$$

Since the upper bound of the conventional TCI depends on the number of variables in the system, Chatziantoniou and Gabauer (2021) propose the corrected Total Connectedness Index (cTCI):

$$cTCI_t = \frac{k}{k-1} TCI_t = \frac{100}{k-1} \sum_{i=1}^{k} \sum_{\substack{j=1 \\ j \neq i}}^{k} \widetilde{\theta}^{g}_{ij,t}(H). \tag{11}$$

The correction rescales the conventional TCI to the 0–100 range without altering the underlying forecast-error variance shares. Since the present system contains eight markets, $k = 8$, and therefore

$$cTCI_t = \frac{8}{7} TCI_t. \tag{12}$$

Accordingly, the corrected TCI is used as the principal measure of system-wide connectedness throughout the study, while the conventional TCI is retained in the connectedness table for comparability with the traditional Diebold–Yilmaz measure.

Finally, net pairwise directional connectedness between markets i and j is defined as

$$NPDC_{ij,t} = 100 \left[\widetilde{\theta}^{g}_{ji,t}(H) - \widetilde{\theta}^{g}_{ij,t}(H) \right]. \tag{13}$$

A positive $NPDC_{ij,t}$ indicates that market i is a net transmitter of shocks to market j, whereas a negative value indicates that market i is a net receiver from market j.

For the average connectedness table, the number of pairwise transmissions (NPT) for market i is defined as

$$NPT_i = \sum_{\substack{j=1 \\ j \neq i}}^{k} \mathbb{I}\left(NPDC_{ij} > 0 \right), \tag{14}$$

where $\mathbb{I}(\cdot)$ is an indicator function equal to one when the condition is satisfied and zero otherwise. NPT therefore records the number of bilateral relationships in which a market is a net transmitter. With eight markets in the system, NPT ranges from zero to seven.

2.2 Maximal Overlap Discrete Wavelet Transform (MODWT)

The maximal overlap discrete wavelet transform, simultaneously localizes signal variations in both time and frequency [1]. This technique decomposes stock index return series at different timescales, utilizing the scaling function (father wavelet, $\varnothing$) and wavelet function (mother wavelet, φ) as noted by Ramsey (2002). Father wavelets represent long-scale smooth components, generating scaling

1. Percival and Walden (2000)

coefficients, while mother wavelets, contributing to differencing coefficients, describe deviations within the smooth components.

We define father wavelet as:

$$\emptyset_{j,k} = -2^{-j/2}\emptyset\left(\frac{t-2^{jk}}{2^j}\right) \text{ with } \int \emptyset(t)dt = 1$$

and mother wavelet as:

$$\varphi_{j,k} = -2^{-j/2}\varphi\left(\frac{t-2^{jk}}{2^j}\right) \text{ with } \int \varphi(t)dt = 0$$

The smooth coefficients generated by father wavelet are defined as:

$$S_{J,k} = \int f(t)\emptyset_{J,k}$$

and detail coefficients generated by mother wavelet as:

$$d_{j,k} = \int f(t)\varphi_{J,k} \text{ with } j = 1, \ldots J$$

The maximal scale of the former is 2^j, while the detailed are computed from the mother wavelets at all scales from 1 to J. The function $f(.)$ from the coefficient above is defined as:

$$f(t) = \sum_k S_{J,k}\emptyset_{J,k}(t) + \sum_k d_{J,k}\varphi_{J,k}(t)\ldots + \sum_k d_{J,k}\varphi_{j,k}(t)\ldots + \sum_k d_{1,k}\varphi_{1,k}(t),$$

which is simplified to

$$f(t) = S_J + D_J + D_{J-1} + \ldots + D_j + \ldots + D_1$$

with orthogonal components defined as:

$$S_J = \sum_k S_{J,k}\emptyset_{J,k(t)}$$

$$D_J = \sum_k d_{J,k}\varphi_{J,k}(t).j = 1, \& \ldots J$$

The resulting multi horizon (multiresolution) breakdown of $f(t)$ is $\left\{S_J, D_{J-1,\ldots,}, D_1\right\}$ .D_j calculates the j th level wavelet detail related to changes in the series at scale $\lambda_{j\ldots}.S_j$ denotes cumulative sum of alterations at each level and as j increases, S_j becomes smoother and smoother (Gençay et al., 2001). MODWT is chosen in the study to estimate scaling and wavelet coefficients due to its superior resolution, avoiding down sampling during coefficient generation. This characteristic facilitates a straightforward comparison between the decomposed and original series, as highlighted by Gençay et al. (2001), Percival and Mofjeld (1997), and Percival (1995). The MODWT does not restrict the sample size to an integer multiple of 2^{J022} unlike the Discrete Wavelet Transform and can be applied to a time series of any length (Percival and Walden, 2000). For decomposition, the study utilises the Daubechies least asymmetric (LA) filter of length eight (LA8) due to its smoother correlation coefficients in contrast to widely applied HAAR wavelet filters, as observed in prior studies (Gençay et al., 2001). The coefficients from the LA (8) filter demonstrate improved uncorrelatedness across scales compared to the HAAR filter [2].

For the empirical analysis, the stock-return series are decomposed using the maximal overlap discrete wavelet transform (MODWT) with a Daubechies least-asymmetric filter of length eight (LA8). Seven detail levels are retained, $J = 7$. Although the sample of $T = 4,520$ observations permits decomposition to additional theoretical levels, seven detail components provide economically interpretable investment horizons extending from 2 to 256 trading days while retaining a sufficiently large number of usable coefficients at the lower-frequency scales.

The resulting decomposition therefore consists of the detail components $D_1, \ldots, D_7$ and the residual smooth component S_7. The detail components correspond approximately to oscillations of 2–4, 4–8, 8–16, 16–32, 32–64, 64–128 and 128–256 trading days, respectively. The smooth component S_7 captures movements at horizons beyond 256 trading days and is not treated as an eighth detail scale. This seven-level specification is used consistently throughout the MODWT decomposition, wavelet multiple correlation and wavelet multiple cross-correlation analyses.

2.3 Continuous Morlet Wavelet Transform (CMWT)

The study employs the Continuous Morlet Wavelet Transform (CMWT), introduced by Morlet et al. (1982), to investigate asset market integration by analysing the wavelet power spectrum and coherence of two signals. CMWT facilitates the isolation and identification of periodic signals while localizing both time and frequency [3]. The estimation of wavelet coherence, cross-correlation, and variance, crucial for assessing co-movements in spatial states, is integral to the study. In their work, In and Kim (2013) define CWMT as the integral over time of the product of the signal and scaled, shifted versions of the wavelet function φ :

$$C(scale, position) = \int_{-\infty}^{\infty} x_t(scale, position, t)dt \tag{15}$$

The results of the Continuous Morlet Wavelet Transform (CMWT) yield several wavelet coefficients, denoted as C, representing scale and position functions that can contain varying values from the time series x_t.The CMWT for two continuous variables is defined by Grossmann and Morlet (1984) as:

$$F(a,b) = \int x_t \varphi\left(\frac{t-a}{b}\right) dt \tag{16}$$

The Morlet wavelet can be simplified as

$$\varphi(\omega) = \pi^{-1/4} e^{i\omega\psi} e^{-\frac{\omega^2}{2}} \tag{17}$$

where, ω is a non-dimensional "time" parameter.

According to Boako and Alagidede (2016), studying the co-movement between two variables entails obtaining a refined version of wavelet coherence through cross-wavelet analysis, wavelet power spectrum, and phase difference. The bivariate cross-wavelet transform (XWT) of x_t and y_t defined by Torrence and Compo (1998) can be written as:

$$W^{xy} = W^x W^{y*} \tag{18}$$

Where W^x and W^y are the respective wavelet transforms which translate the Fourier co- and quadrature-spectra into frequency time domain (Roesch et al., 2014). In line with Veleda et al. (2012),

2. Cornish et al. (2006)
3. Grinsted et al. (2004)

the wavelet power spectrum describes the local covariance between two time series, which is specified as:

$$P^{xy}(s,\tau) = \left|W^{xy}(s,\tau)\right| \tag{19}$$

where s is the frequency and τ is the time. The challenge in assessing the degree of integration of two series posed by the wavelet power spectrum is addressed through wavelet coherency, as highlighted by Roesch et al. (2014). As noted by Torrence and Webster (1999), wavelet coherence serves as the local correlation coefficient in the time-frequency space, analogous to the traditional correlation coefficient. We specify the wavelet coherence of two time series x_t and y_t as:

$$R_t^2 = \frac{\left|S\left(W_t^{xy}\right)(s)\right|^2}{S\left(s^{-1}\left|W_t^x(s)\right|^2\right)\cdot S\left(s^{-1}\left|W_t^y(s)\right|^2\right)} \tag{20}$$

where S is a smoothing operator. Wavelet coherence close to one between two time series signifies a high level of integration, while coherence close to zero indicates no integration between the series. Madaleno and Pinho (2012) describe the wavelet phase as a representation that reveals lead (lag) associations between two time series at various frequencies:

$$\theta_{xy} = \tan^{-1}\frac{I\left\{W_t^{xy}\right\}}{\Re\left\{W_t^{xy}\right\}}, \theta_{xy} \in [-\pi,\pi] \tag{21}$$

Two series are considered to be in-phase (out of phase) when the absolute value of θ_{xy} less (greater) than $\pi/2$. The concept refers to the instantaneous time as the time origin and applies to the frequency under consideration. Additionally, the arrows of the phase indicate which series leads in the relationship.

2.4 The Wavelet Multiple Correlation and Wavelet Multiple Cross-Correlation

In the multivariate collection of distinct time scales for diverse stock market returns, the wavelet multiple correlations (WMC) and wavelet multiple cross-correlations (WMCC) allow for multiple correlations and cross-correlations, as stated by Fernández-Macho (2012). Type 1 errors and spurious correlations are both mitigated by this method.

The WMC and WMCC commence with the definition of the maximal overlap discrete wavelet transform (MODWT) as follows: Let $X_t = x_{1t}, x_{2t}, \ldots, x_{nt}$ represent a multivariate stochastic process and $W_{jt} = w_{1jt}, w_{2jt}, \ldots, w_{njt}$ denote the corresponding scale λ_j wavelet coefficients obtained through the application of MODWT. The wavelet multiple correlations $(WMC)\varphi X\left(\lambda_j\right)$ can be expressed as a singular set of multiscale correlations from Eq. (8) subsequently

$$\varphi X\left(\lambda_j\right) = \sqrt{1-\frac{1}{\text{maxdiag}\, P_j^{-1}}} \tag{22}$$

For each λ_j the square roots of the regression coefficients of determination are derived by the linear combination of $w_{ijt}, i = 1,2,\ldots,n$ variables, selecting those for which the coefficient of determination is maximum. Prior studies indicate that, in regression of a regressand z_t on a set of predictors $z_t\{z_k, k \neq 1\}$ the coefficient of determination can be computed as $R_i^2 = 1 - 1/\rho^{ii}$, i^{th} diagonal element of the inverse of the complete correlation matrix P where P_j is the $(n\times n)$ correlation matrix of $\mathrm{W}_{jt} = w_{1jt}, w_{2jt}, \ldots, w_{njt}$ and max diag (.) selects the maximum element in the diagonal argument.

From the regression theory; the fitted values of z_i as $\hat{z}_i$ WMC can also be expressed as Eq. (9), where w_{ij} is chosen to maximise $\varphi X\left(\lambda_j\right)$ and $\hat{w}_{ijt}$ are the fitted values in the regression of w_{ij} on the rest of the wavelet coefficients at scale λ_j

$$\varphi X\left(\lambda_j\right)=\frac{\operatorname{Corr}\left(w_{ijt},\frown w_{ijt}\right)\operatorname{Cov}\left(w_{ijt},\frown w_{ijt}\right)}{\sqrt{\operatorname{Var}\left(w_{ijt}\right)\operatorname{Var}\left(\frown w_{ijt}\right)}} \tag{23}$$

In accordance with the methodology outlined by Gençay et al. (2001), the wavelet covariances and variances can be estimated as

$$\operatorname{Var}\left(\tilde{w}_{ijt}\right)=\bar{\delta}_j^2=\frac{1}{\tilde{T}_j}\sum_{t=:j-1}^{T-1}\tilde{w}_{ijt}^2 \tag{24}$$

$$\operatorname{Var}\left(\tilde{\tilde{w}}_{ijt}\right)=\bar{\vartheta}_j^2=\frac{1}{\tilde{T}_j} \tag{25}$$

$$\operatorname{Cov}\left(\tilde{w}_{ijt},\widetilde{w}_{ijt}\right)=\bar{\gamma}_j=\frac{1}{\tilde{T}_j}\sum_{t=L_j-1}^{T-1}\tilde{w}_{ijt}^2\widetilde{w}_{ijt} \tag{26}$$

where $\tilde{w}_{ij}$ represents the scenario where the regression of the same on the set of regressors $\left\{\tilde{w}_{kj},k\neq i\right\}$ maximises the coefficient of determination, $\widetilde{w}_{ij}$ denotes corresponding fitted values, and $L_j=\left(2^j-1\right)(L-1)$ is the number of wavelet coefficients affected by the boundary conditions associated with wavelet filter of length L and scale λ_j whereas $\tilde{T}=T-L_j+1$ is the number of wavelet coefficients unaffected by the boundary conditions. In the empirical implementation, boundary-affected MODWT coefficients are removed using the brick-wall boundary treatment. For the LA8 filter, $L=8$, and the number of boundary-affected coefficients at detail level j is

$$L_j=(2^j-1)(L-1).$$

The empirical number of usable coefficients is therefore $T-L_j$. With $T=4,520$, this produces 4,513, 4,499, 4,471, 4,415, 4,303, 4,079 and 3,631 usable coefficients for D_1 through D_7, respectively. This boundary treatment is applied consistently before estimation of the WMC and WMCC statistics.

Similar, a consistent estimator of the wavelet multiple cross-correlation can be calculated as

$$\varphi X,\tau\left(\lambda_j\right)=\frac{\operatorname{Corr}\left(\tilde{w}_{ijt},\widetilde{w}_{ijt+\tau}\right)\operatorname{Cov}\left(\tilde{w}_{ijt},\tilde{\tilde{w}}_{ijt+\tau}\right)}{\sqrt{\operatorname{Var}\left(\tilde{w}_{ijt}\right)\operatorname{Var}\left(\widetilde{w}_{ijt+\tau}\right)}} \tag{27}$$

The confidence intervals are constructed using the transformation defined by Fisher (1915) as $\arctan h(r)$, where $\arctan h(*)$ represents the inverse hyperbolic tangent function.

The confidence intervals is constructed on the assumption that $X_1\ldots.X_T$ is the realisation of X in the estimation of wavelet multiple correlation and cross-correlation and hence for $X\left(\lambda_j\right)$ in (2.15) then $\tilde{z}_j\sim F\mathcal{N}\left(z_j,\left(T/2^j-3\right)^{-1}\right)$ where $z_j=\arctan h\left(\varphi X\left(\lambda_j\right)\right)$, $\tilde{z}_j=\arctan h\left(\tilde{\varphi}X\left(\lambda_j\right)\right)$, and $F\aleph$ symbolise the folded normal distribution. Therefore, an approximate $(1-\alpha)$CI for the true value of

WMC is given by $CI_{(1-\alpha)}\left(\varphi X\left(\lambda_j\right)\right) = \tanh\left[\tilde{z}_j - \frac{c_2}{\sqrt{T/2^j-3}}; \tilde{z}_j + \frac{c_1}{\sqrt{T/2^j-3}}\right]$ where the $F\aleph$ critical values c_1, c_2 are such that $\phi\left(c_1\right) + \phi\left(c_1 - 2z^0\right) = 1 - \alpha/2$ and $\phi\left(c_2\right) + \phi\left(c_1 - 2z^0\right) = 2 - \alpha/2$ with ϕ as the standard Gaussian probability distribution function and $\tanh\left(z^0\right) = \varphi_X^0(\lambda)$ as the value of some wavelet multiple correlation as set under certain null hypothesis of no correlation. For a comprehensive understanding of wavelet-based methods, there are a number of studies (Fernández-Macho, 2012; Carmona et al., 1998; In and Kim, 2013; Tiwari et al., 2013; Nason, 2008). Throughout the empirical discussion, the terms 'transmitter', 'receiver', 'leadership' and 'spillover' refer to directional statistical connectedness within the estimated system. They are not interpreted as structurally identified causal effects unless explicitly stated otherwise.

3. Data description and statistical properties

To investigate South Africa's integration with G7 stock markets, we employ bivariate (cross-wavelet coherency and phase difference) and multivariate (wavelet multiple correlation and wavelet multiple cross-correlation) methods on eight stock indices: JSE (South Africa), SP500 (US), DAX (Germany), FTALLSH (United Kingdom), TSX60 (Canada), CAC40 (France), MIB (Italy), and NIKKEI225 (Japan). Daily closing market indices from July 3, 2006, to October 27, 2023, sourced from Thomson Reuters Datastream, are expressed in USD for uniformity, mitigating exchange rate noise (Pukthuanthong and Roll, 2009). Monday-to-Friday returns are calculated due to non-trading on weekends, and non-synchronous data points are removed to avoid underestimating true correlations (Martens and Poon, 2001), resulting in 4520 observations. After converting daily price data to returns, summary statistics indicate SP500 with higher average returns and JSE with notable volatility. Except for Italy (MIB) and the United Kingdom (FTALLSH), all markets show positive average returns. From table 1 we observe that South Africa (JSE) exhibits the highest standard deviation, signifying the most volatility, while the US (SP500) has the lowest standard deviation, indicating the least volatility. Returns for South Africa and G7 display negative skewness, suggesting a prevalence of negative returns. Leptokurtosis, heavy-tails, and high peaks in all return series indicate asymmetry and non-normality. Pictorial representations of SA and G7 stocks returns exhibit fat tails, volatility clustering, and asymmetry, justifying the application of wavelet techniques to model returns and assess their integration across

Table 1. Summary statistics of stock markets of South Africa and G7 countries

Index	Mean (10^{-5})	Std. Dev. (10^{-5})	Skewness	Ex. Kurtosis	JB
SP500	0.2601	0.393700	-0.524	12.783	30980.7
DAX	0.1680	0.492950	-0.222	8.049	12238.5
CAC40	0.0275	0.502991	-0.225	8.594	13947.1
MIB	-0.1100	0.563028	-0.596	9.370	16803.4
FTALLSH	-0.0310	0.427785	-0.585	10.809	22261.6
TSX60	0.0715	0.447214	-0.945	15.285	44672.8
JSE	0.0477	0.575326	-0.345	5.014	4824.8
NIKKEI225	0.0936	0.431277	-0.295	6.346	7649.7

Notes: JB denotes the Jarque–Bera statistic for normality. Std. Dev. denotes standard deviation.

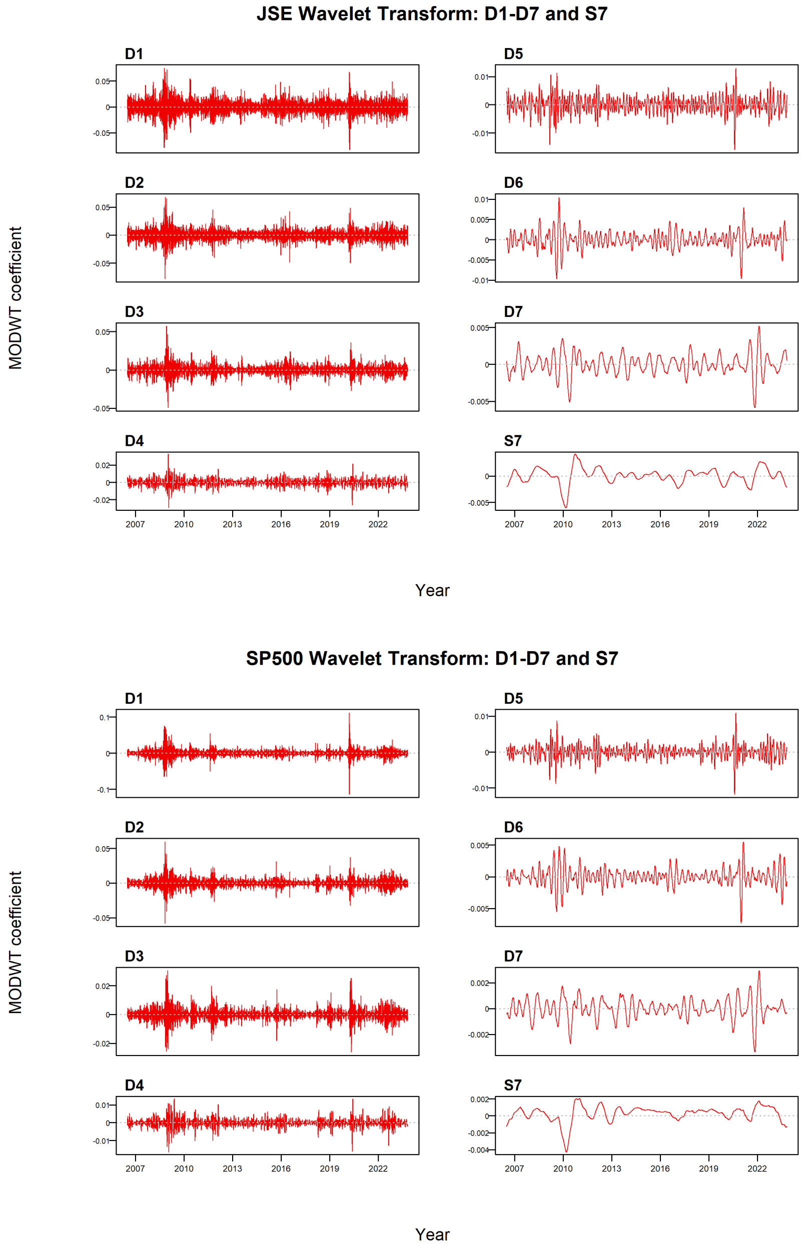

JSE and S&P 500

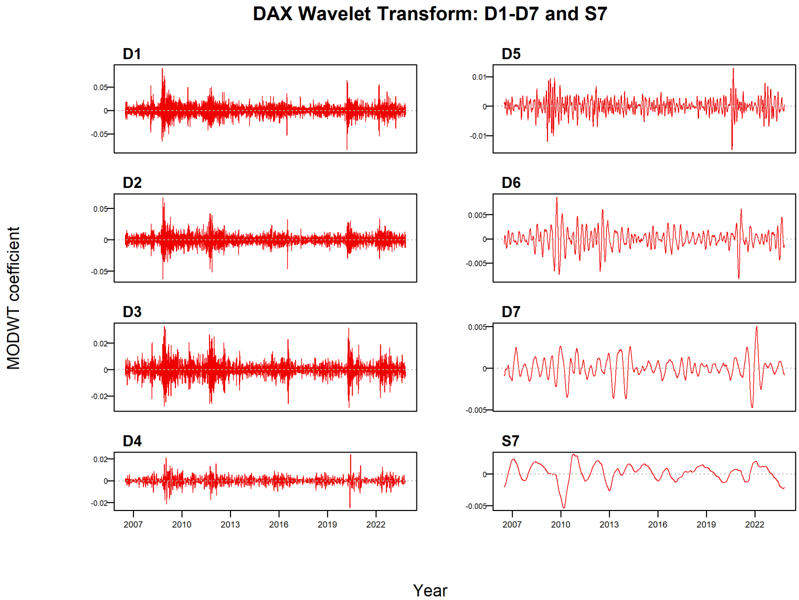

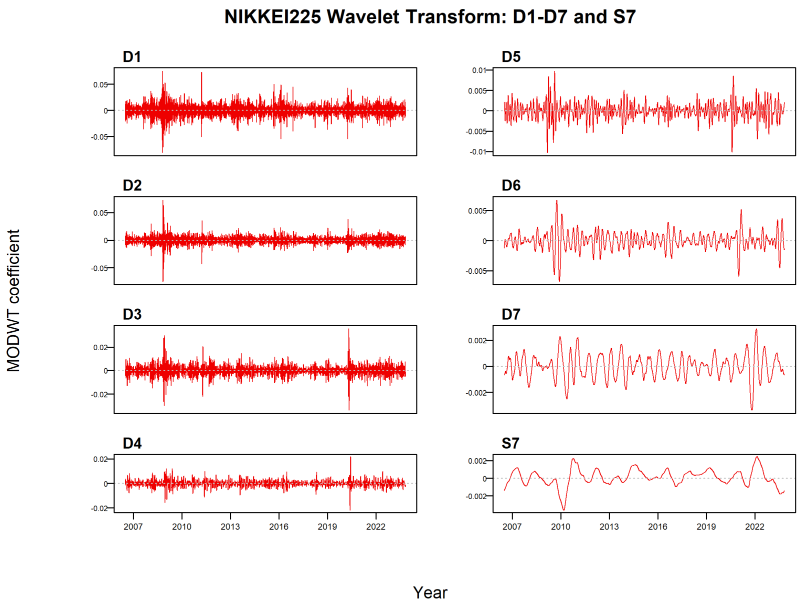

DAX and NIKKEI 225

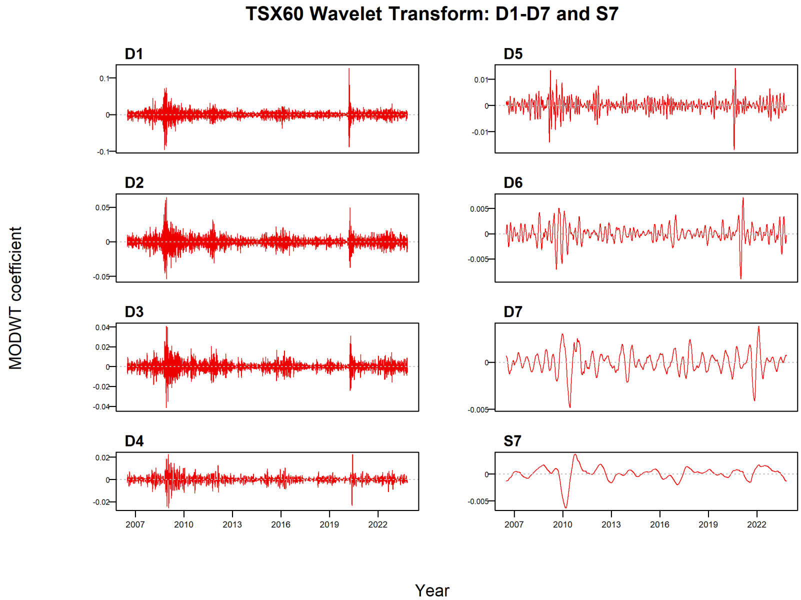

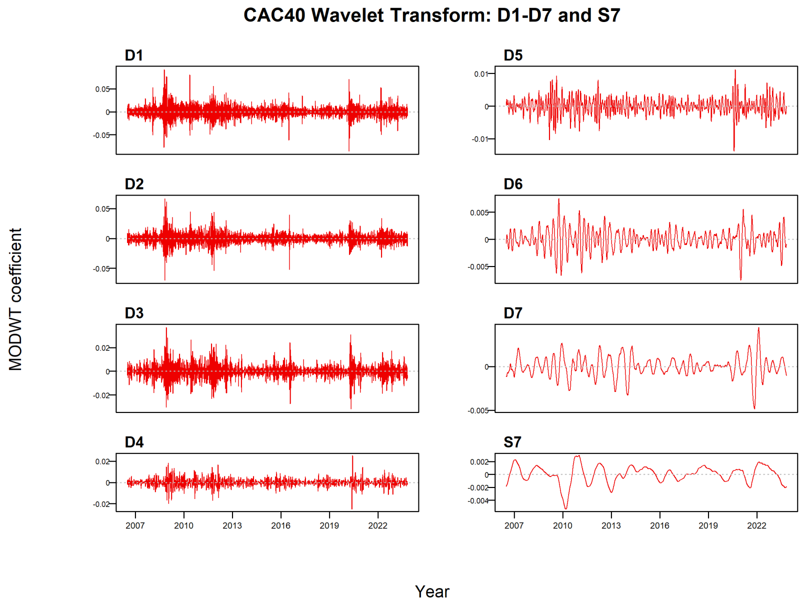

TSX 60 and CAC 40

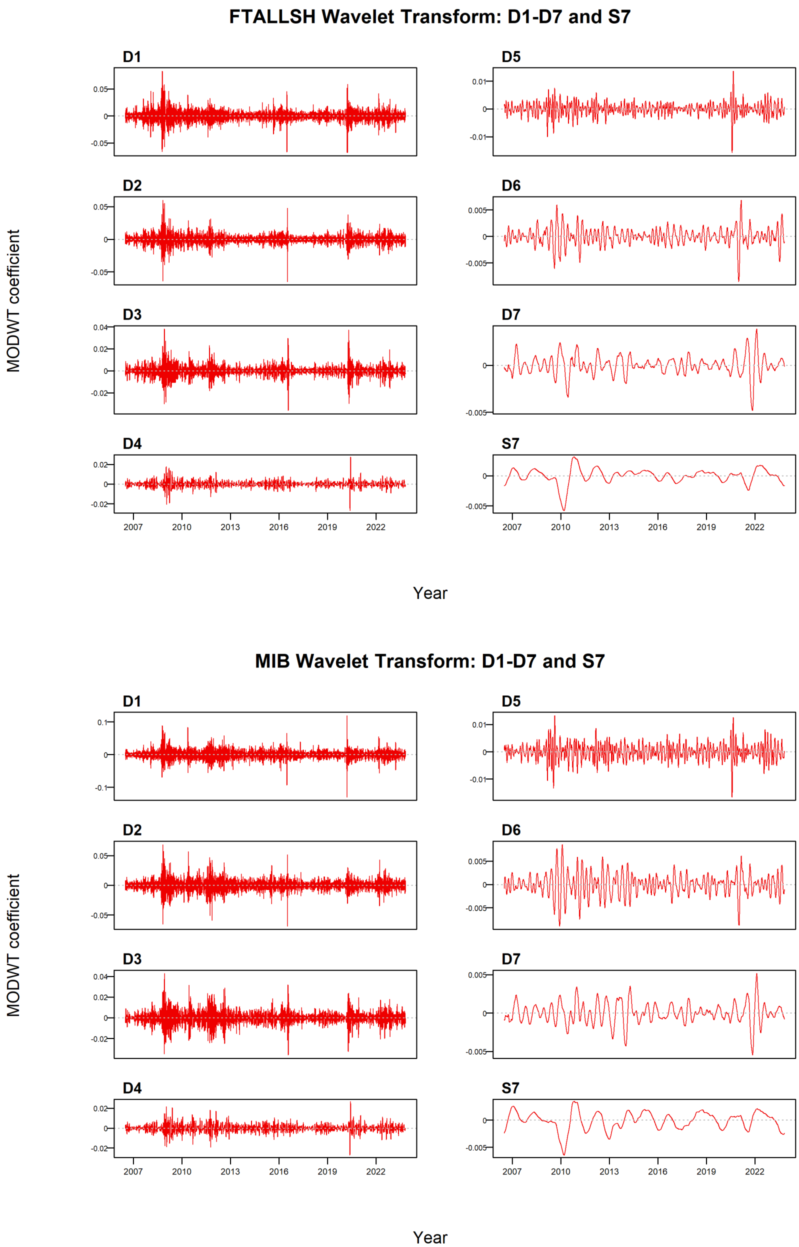

Figure 1. MODWT decomposition of South African and G7 stock market returns. Each return series is decomposed using the LA8 filter into seven detail components, D_1–D_7, corresponding approximately to 2–4, 4–8, 8–16, 16–32, 32–64, 64–128, and 128–256 trading days, respectively. The S_7 component represents the smooth component at horizons beyond 256 trading days.

4. Results and discussion

This section presents the results of the study, structured into two primary analyses, (1) the time-varying connectedness and (2) the wavelet-based co-movement analysis. First, we discuss the findings from the time-varying parameter vector autoregressive model (TVP-VAR), which examines the average and dynamic total connectedness measures, net total connectedness and pairwise dynamic connectedness among stock markets, highlighting key patterns of shock transmission across different financial crises. This is followed by the wavelet analysis, which provides a multi-scale perspective on stock market integration. Specifically, we explore the bivariate co-movement between the South African stock market (JSE) and G7 markets, before extending the analysis to multivariate relationships using wavelet multiple correlation (WMC) and wavelet multiple cross-correlation (WMCC).

4.1 Average and dynamic total connectedness measures

Table 2 reports the average connectedness measures for the South African and G7 equity markets. The ordinary Total Connectedness Index is 73.06%, while the corrected TCI is 83.49%, indicating substantial cross-market dependence within the estimated system. Gross outward connectedness is highest for the CAC40 (99.06), DAX (94.34), FTALLSH (88.68) and MIB (85.21). Net connectedness provides the more appropriate measure for identifying persistent transmitting and receiving positions. On this basis, the CAC40 is the strongest net transmitter, with a NET value of 20.17, followed by the DAX (16.22), FTALLSH (11.78) and MIB (8.60). In contrast, the JSE (-8.11) and NIKKEI225 (-53.79) are net receivers within the estimated network.

For South Africa specifically, the system-wide transmitter ranking does not map directly onto the JSE's average forecast-error variance exposure. The largest contributions to JSE forecast-error variance originate from FTALLSH (14.11%), CAC40 (13.17%), DAX (12.60%), TSX60 (11.55%) and MIB (10.84%), compared with 8.23% from the S&P 500 and 1.63% from NIKKEI225. This distinction is central to the paper: the market occupying the strongest transmitting position in the full network need not be the market accounting for the largest average share of JSE forecast-error variance.

Dynamic connectedness in Figure 2 exhibits substantial variation through time, with the TCI rising above 90% around the Global Financial Crisis, the euro-area debt crisis and the COVID-19 pandemic. The highest observed TCI occurs around the COVID-19 episode, while a more moderate increase is visible around the onset of the Russia–Ukraine war. Connectedness declines noticeably around late 2012 and again around 2017 before subsequently increasing.

These crisis-related patterns are interpreted descriptively. Because the analysis does not impose ex ante event windows or formally test differences between crisis and non-crisis periods, the observed peaks should not be interpreted as statistically established crisis effects. Moreover, the estimated connectedness may reflect both bilateral market relationships and common exposure to global financial conditions.

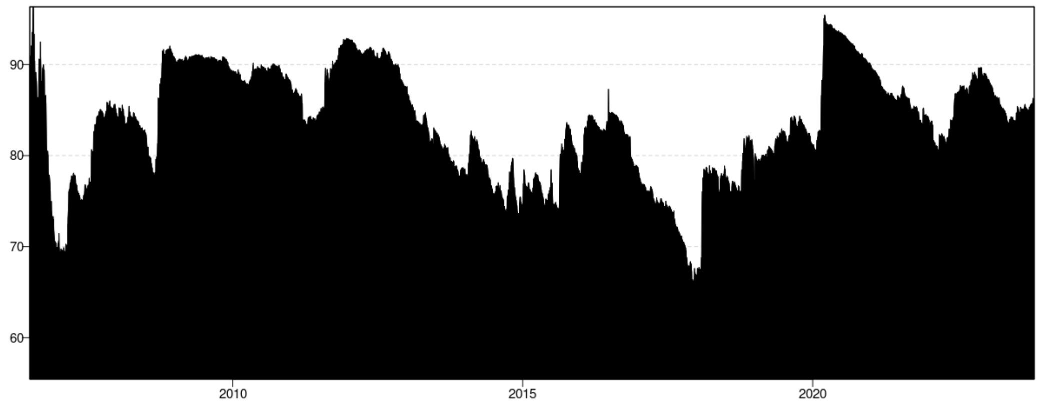

Figure 2. Dynamic Total Connectedness. Results are derived using a TVP-VAR model with a lag length of one (BIC) and a 20-step-ahead generalized forecast error variance decomposition.

4.2 Net total connectedness

Figure 3 reports the time-varying net directional connectedness of each equity market, defined as the difference between outward and inward directional connectedness within the estimated system. Positive values identify net transmitting positions, while negative values identify net receiving positions.

The JSE is predominantly a net receiver over the sample period, with more pronounced negative positions visible around 2008–2009, 2014–2015, 2020 and early 2022. By contrast, the CAC40, DAX, FTALLSH and MIB generally maintain positive net positions, consistent with their positive average NET measures reported in Table 2. Economically, this suggests that South Africa is more often positioned on the receiving side of international equity-market dependence, whereas several European markets occupy more persistent transmitting positions.

These classifications should nevertheless be interpreted as properties of the estimated directional connectedness network rather than as evidence of structurally identified causal transmission, since common global factors may contribute to the observed relationships.

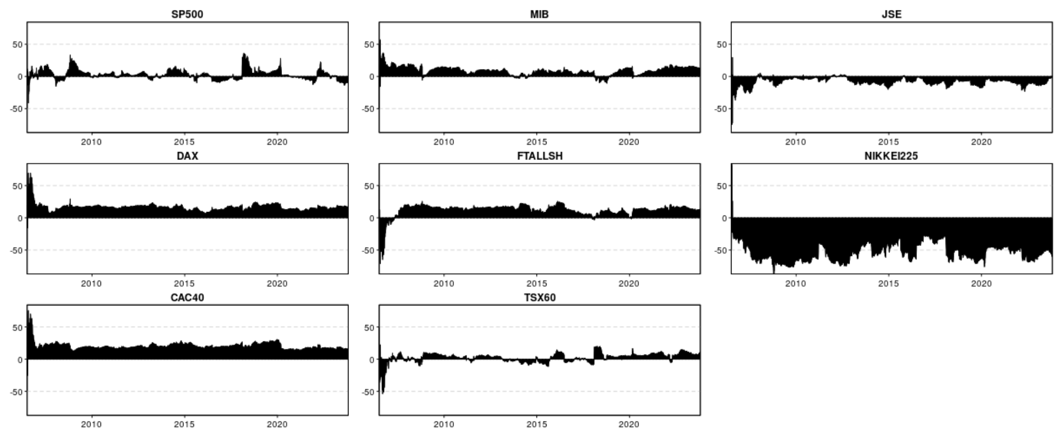

Figure 3. Net total directional connectedness. Results are derived using a TVP-VAR model with a lag length of one (BIC) and a 20-step-ahead generalized forecast error variance decomposition.

4.3 Net pairwise dynamic connectedness measure

Net directional connectedness identifies whether a market occupies a net transmitting or receiving position within the overall system, but aggregate measures may conceal important bilateral relationships. Figure 4 therefore reports net pairwise dynamic connectedness between the JSE and individual G7 markets.

The S&P 500 generally occupies a net transmitting position relative to the JSE, with bilateral connectedness rising sharply around the COVID-19 episode and reaching its highest observed level just below 80%. NIKKEI225, by contrast, is predominantly a net receiver relative to the JSE. Several European markets, together with the United Kingdom and Canada, display stronger average bilateral connectedness with South Africa than the United States over extended parts of the sample. These findings reinforce the broader result that the identity and strength of the markets most closely associated with JSE movements vary through time.

The episode-specific increases are interpreted descriptively because the analysis does not formally test differences across predetermined crisis and non-crisis windows. In addition, net pairwise connectedness measures directional statistical dependence rather than structurally identified direct transmission, and the estimated relationships may partly reflect common exposure to global risk factors.

	SP500	DAX	CAC40	MIB	FTALLSH	TSX60	JSE	NIKKEI225	FROM
SP500	32.44	11.06	11.53	9.53	11.47	15.94	6.95	1.09	67.56
DAX	8.66	21.88	19.22	16.38	13.70	8.84	9.90	1.43	78.12
CAC40	8.72	18.65	21.11	16.94	14.15	9.09	10.02	1.32	78.89
MIB	7.76	17.58	18.75	23.39	13.52	8.71	9.17	1.11	76.61
FTALLSH	9.80	14.44	15.43	13.35	23.10	10.98	11.69	1.21	76.90
TSX60	14.47	10.80	11.45	9.94	12.71	28.60	10.77	1.26	71.40
JSE	8.23	12.60	13.17	10.84	14.11	11.55	27.87	1.63	72.13
NIKKEI225	12.67	9.22	9.51	8.22	9.02	8.67	5.53	37.16	62.84
TO	70.31	94.34	99.06	85.21	88.68	73.79	64.02	9.05	584.44
Inc.Own	102.74	116.22	120.17	108.60	111.78	102.39	91.89	46.21	CTCI/TCI
NET	2.74	16.22	20.17	8.60	11.78	2.39	-8.11	-53.79	83.49 / 73.06
NPT	2.00	6.00	7.00	4.00	5.00	3.00	1.00	0.00	

Table 2. Notes: Results are based on a TVP-VAR model with lag length one (BIC) and a 20-step-ahead generalized forecast error variance decomposition.

4.4 Wavelet Analysis

To examine horizon-specific dependence between South Africa and the G7 markets, we first analyse bilateral JSE–G7 relationships using cross-wavelet coherence and phase differences and then examine multivariate dependence using wavelet multiple correlation (WMC) and wavelet multiple cross-correlation (WMCC). For the multivariate analysis, daily stock returns are decomposed using a seven-level MODWT with a Daubechies least-asymmetric filter of length eight (LA8).

The retained detail components D_1–D_7 correspond approximately to 2–4, 4–8, 8–16, 16–32, 32–64, 64–128 and 128–256 trading days, respectively. The residual smooth component S_7 represents movements beyond 256 trading days and is not treated as an additional detail scale. Table 3 summarises the scale definitions used throughout the empirical analysis.

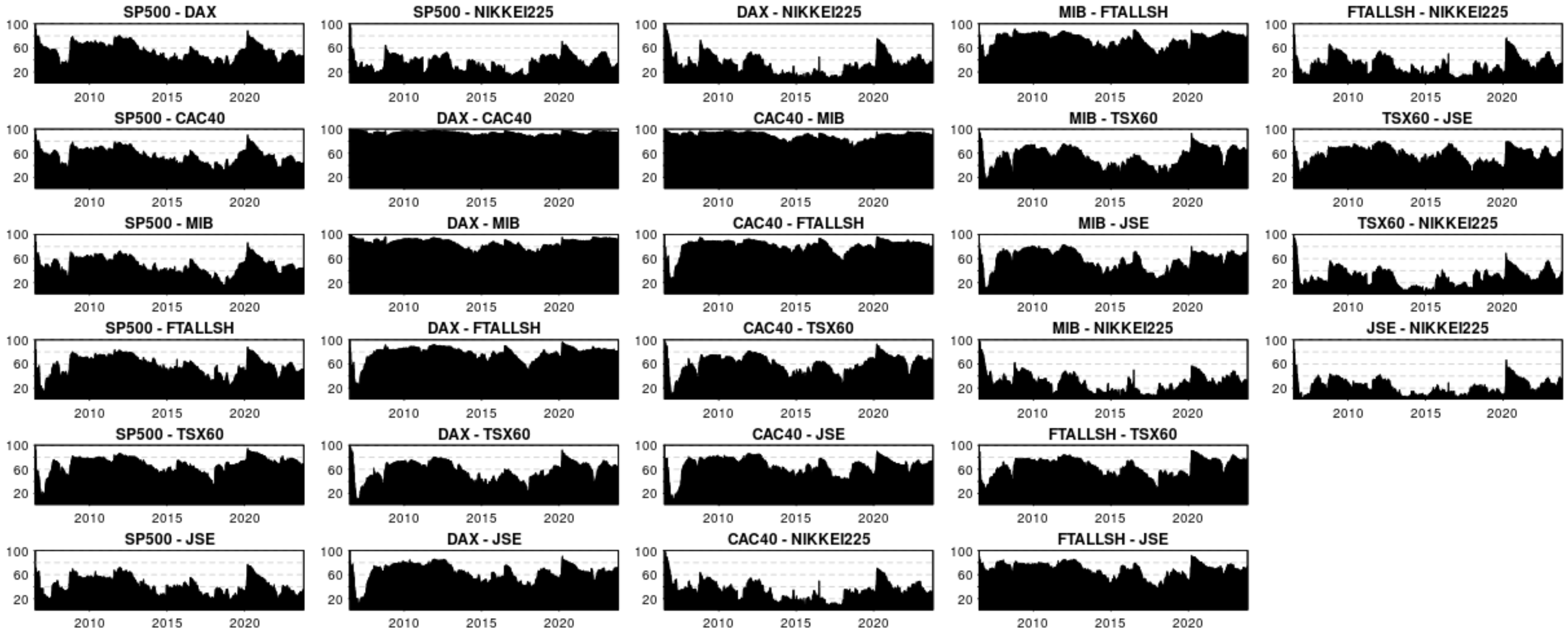

Figure 4. Net pairwise directional connectedness. Results are obtained from a TVP-VAR model with one lag selected by BIC and a 20-step-ahead generalized forecast error variance decomposition.

Table 3. MODWT detail levels and investment horizons

Component	Approximate horizon	Investment-horizon classification
D_1	2–4 trading days	Short term
D_2	4–8 trading days	Short term
D_3	8–16 trading days	Short term
D_4	16–32 trading days	Medium term
D_5	32–64 trading days	Medium term
D_6	64–128 trading days	Long term
D_7	128–256 trading days	Long term
S_7	> 256 trading days	Residual smooth component

4.4.1 Bivariate co-movement between Returns on South African and G7 stocks

Figure 5 presents the cross-wavelet coherency results for South Africa–G7 stock market pairs, illustrating pairwise integration in the time–frequency domain. Wavelet coherency measures local correlation across short-, medium-, and long-term horizons, while phase-difference arrows indicate lead–lag relationships. Overall, the results reveal substantial co-movement between South Africa and G7 equity markets, with integration predominantly concentrated at medium and long horizons. Strong coherency within the cone of influence suggests that co-movement is economically meaningful, while weaker short-horizon integration indicates heterogeneous high-frequency dynamics. The variability of phase-difference vectors across time confirms that lead–lag relationships are non-uniform and horizon-dependent.

At the bilateral level, the SP500–JSE pair exhibits strong medium- to long-term integration (16–64 days), with the S&P 500 consistently leading the JSE between 2007 and early 2012, while short-term integration remains limited. A similar pattern is observed for the FTALLSH–JSE pair, where pronounced medium-term co-movement (32–64 days) and clear UK market leadership are evident from 2006 to 2009. These dynamics reflect South Africa's deepening trade openness, financial liberalisation, and strong economic linkages with advanced economies.

European markets display pronounced but episodic influence on South Africa. The DAX–JSE and CAC40–JSE pairs show strong medium- and long-term integration during crisis periods (2007–2010), with German and French markets leading the JSE, but integration weakens markedly between 2013 and 2019, aside from isolated volatility episodes. The MIB–JSE relationship exhibits semi-strong medium- to long-term co-movement during 2007–2010, with Italy leading South Africa, though long-run integration declines thereafter. In contrast, the NIKKEI225–JSE pair shows persistently weak integration, with only sporadic long-horizon co-movement during major global crises.

Taken together, the bivariate wavelet evidence indicates that South Africa's stock market is primarily influenced by U.S. and European markets at medium and long horizons, while short-term integration remains limited and uneven. These findings reinforce the importance of accounting for scale-dependent dynamics when assessing international market integration and diversification potential.

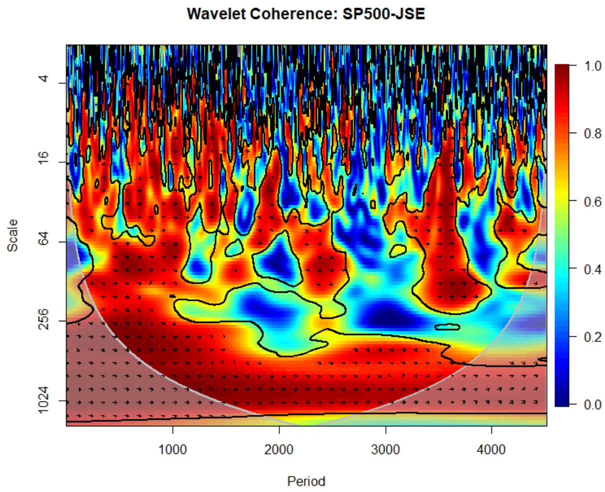

Time Index	Date
1000	April 2010
2000	August 2014
3000	January 2019
4000	June 2022

Table 4. Legend: Time scale reference for cross-wavelet coherency

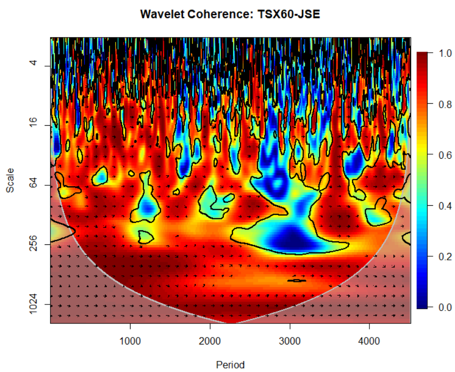

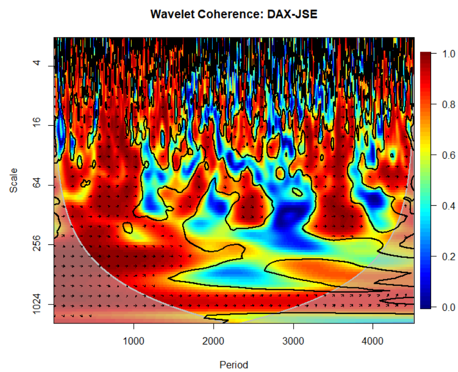

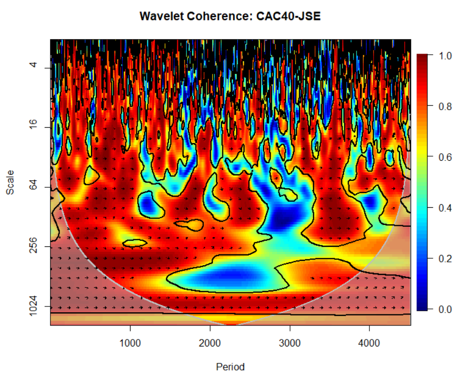

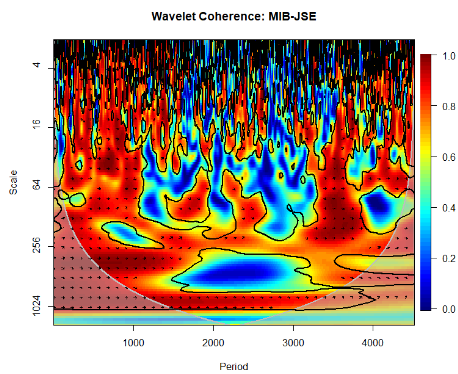

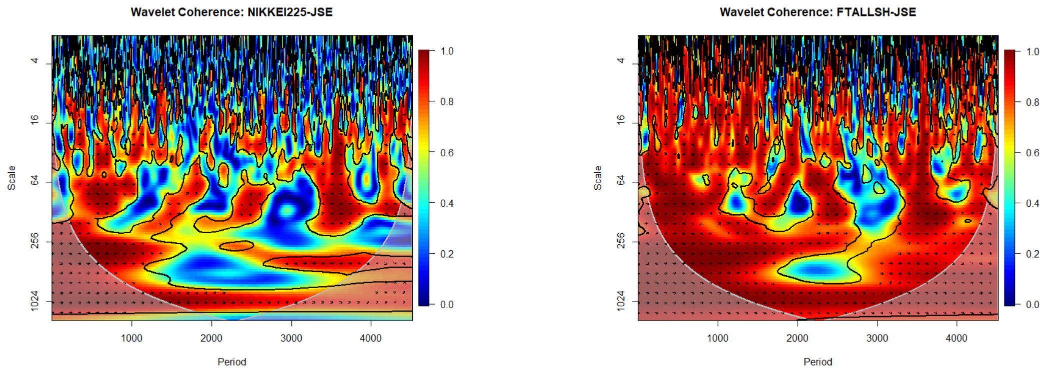

Figure 5. South Africa–G7 stock market cross-wavelet coherency

4.4.2 Multivariate co-movement of stock returns between South Africa and G7

To assess multivariate dependence across South African and G7 equity markets, we estimate wavelet multiple correlation (WMC) and wavelet multiple cross-correlation (WMCC) using the seven MODWT detail components D_1–D_7. These correspond to approximately 2–4, 4–8, 8–16, 16–32, 32–64, 64–128 and 128–256 trading days.

For interpretation, D_1–D_3 represent short-term horizons of approximately 2–16 trading days, D_4–D_5 represent medium-term horizons of approximately 16–64 trading days, and D_6–D_7 represent long-term horizons of approximately 64–256 trading days. The smooth component S_7, which captures fluctuations beyond 256 trading days, is not included as an additional WMC or WMCC detail scale.

4.4.3 WMC for South Africa and G7 stock returns

Figure 7 reports the wavelet multiple correlation (WMC) results for the South African and G7 equity markets across the seven MODWT detail levels. Multivariate dependence is persistently high across all investment horizons. The estimated WMC increases from 0.966 at D_1 to 0.970 at D_2, 0.974 at D_3 and D_4, before declining slightly to 0.972 at D_5. It subsequently rises to 0.978 at D_6 and remains approximately 0.977 at D_7. The variation across scales is therefore modest and not strictly monotonic. The principal finding is consequently the persistence of very strong multivariate co-movement across investment horizons rather than a sharp transition from weak short-run to strong long-run integration.

The CAC40 is the maximizing market at every detail level, D_1–D_7. In the WMC framework, this means that the CAC40 wavelet component exhibits the highest multiple correlation with a linear combination of the remaining markets at each scale. This finding identifies France as the market most closely aligned with the common multivariate component of the South Africa–G7 system, but it should not be interpreted as evidence that the French market is the direct causal source of JSE movements.

The persistence of the CAC40 as the maximizing market also requires economic caution. Since France, Germany and Italy share common euro-area monetary and financial conditions, and all indices in the study are expressed in U.S. dollars, some of the measured multivariate dependence may reflect common regional, currency and global-factor exposure rather than bilateral market-to-market transmission. The WMC evidence is therefore interpreted as evidence of strong system-wide multivariate dependence across investment horizons.

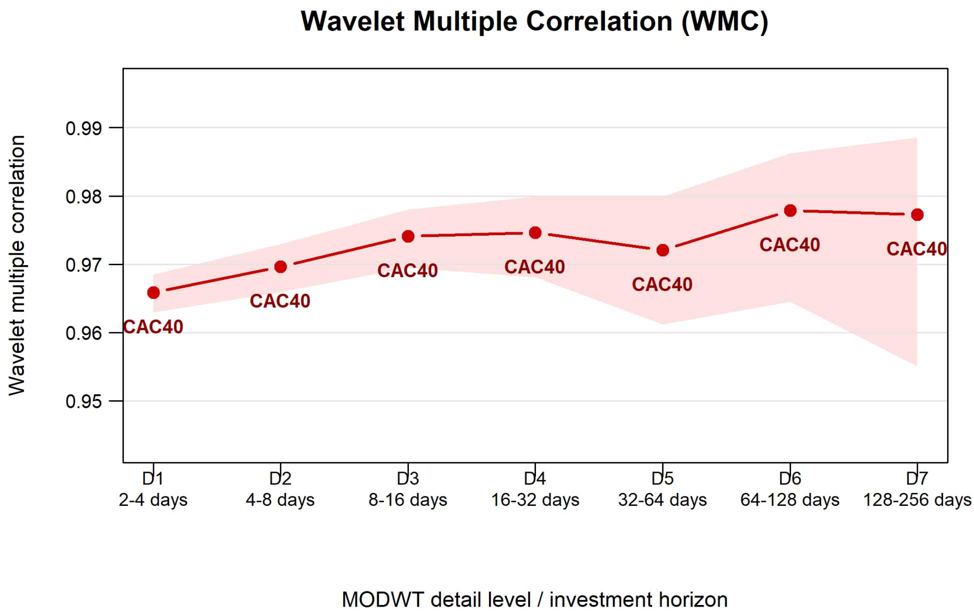

Figure 7. Wavelet multiple correlation (WMC) across South African and G7 equity markets. Results are reported for the seven MODWT detail levels D_1–D_7, corresponding approximately to 2–4, 4–8, 8–16, 16–32, 32–64, 64–128 and 128–256 trading days, respectively. The shaded area represents the 95% confidence interval. The market label identifies the variable that maximizes the multiple correlation at each scale. CAC40 is the maximizing market at all seven detail levels.

4.4.4 WMCC for South Africa and G7 stock returns

Figure 8 reports wavelet multiple cross-correlation (WMCC) across the South African and G7 equity markets over leads and lags of up to 30 trading days. At each detail level, WMCC identifies the market whose wavelet component maximizes cross-correlation with a linear combination of the remaining markets. Under the adopted sign convention, a negative maximizing lag indicates that the selected market leads the linear combination of the remaining markets, a positive lag indicates that it follows, and zero denotes contemporaneous dependence.

The CAC40 is the maximizing market at all seven detail levels, consistent with the WMC results. At D_1, D_2, D_3, D_4, D_5 and D_7, the maximum occurs at zero lag. These results indicate that the strongest multivariate dependence is predominantly contemporaneous at horizons of 2–64 trading days and 128–256 trading days. At D_6, corresponding to approximately 64–128 trading days, the maximum occurs at a one-day negative lag. Under the stated convention, this means that the CAC40 leads the linear combination of the remaining markets by approximately one trading day at this horizon.

The corrected WMCC evidence therefore does not support a rotation toward different multivariate leaders as the investment horizon increases. Instead, the CAC40 remains the maximizing market throughout the seven-level scale domain, while a measurable temporal lead emerges only at D_6. This distinction is important because the WMCC statistic identifies system-level predictive lead–lag dependence rather than structurally identified causal transmission to the JSE. The prominence of CAC40 may additionally reflect exposure to common euro-area, currency and global financial factors. Accordingly, the D_6 result is interpreted as evidence of horizon-specific multivariate leadership within the estimated system rather than direct causal transmission from France to South Africa.

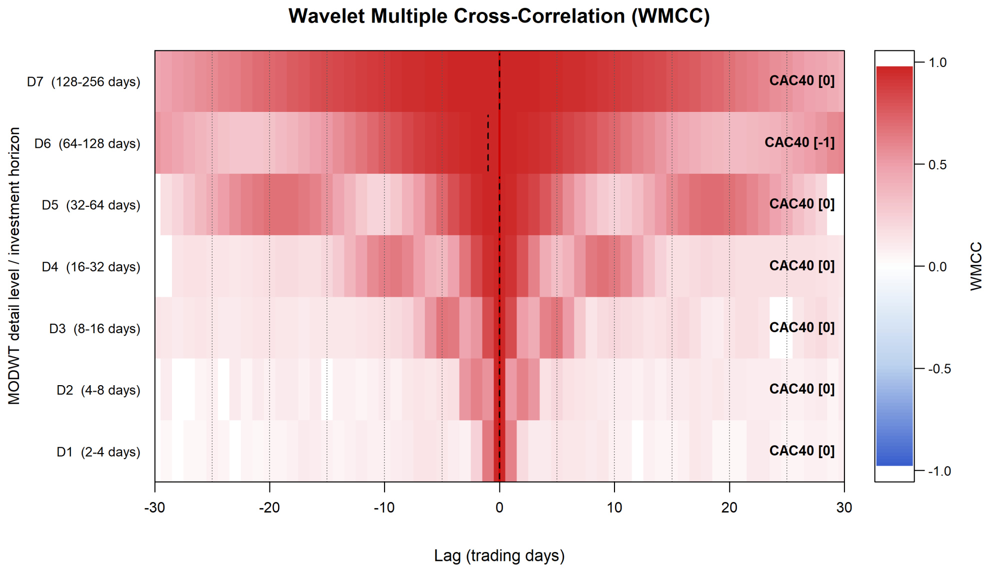

Figure 8. Wavelet multiple cross-correlation (WMCC) across South African and G7 equity markets over leads and lags of up to 30 trading days. Results are reported for the seven MODWT detail levels D_1–D_7, corresponding approximately to 2–4, 4–8, 8–16, 16–32, 32–64, 64–128 and 128–256 trading days, respectively. Labels identify the market that maximizes the multiple cross-correlation at each scale, with the corresponding peak lag reported in square brackets. Negative lags indicate that the maximizing market leads the linear combination of the remaining markets, positive lags indicate that it follows, and zero denotes contemporaneous dependence. White regions indicate areas where the 95% confidence interval includes zero.

5. Conclusions and policy implications

This study investigated the dynamic interconnectedness between South Africa's stock market and G7 equity markets using daily stock index returns from 3 July 2006 to 27 October 2023. The analysis covered South Africa (JSE) and seven G7 markets, S&P 500, FTALLSH, DAX, CAC40, MIB, TSX, and NIKKEI 225. To capture both evolving spillovers and horizon-specific integration, the study combined a Time-Varying Parameter Vector Autoregressive (TVP-VAR) connectedness framework with wavelet-based methods, including cross-wavelet coherency, phase difference analysis, wavelet multiple correlation (WMC), and wavelet multiple cross-correlation (WMCC). This integrated framework allowed simultaneous examination of when shocks propagate and over which horizons integration strengthens or weakens.

The TVP-VAR results reveal a high degree of time-varying interconnectedness between South Africa and G7 stock markets, with crisis periods acting as catalysts for intensified spillovers. The net directional connectedness analysis identifies the S&P 500 as a dominant emitter of shocks to the JSE over the full sample, with spillover intensity peaking just below 80% during the COVID-19 pandemic. Among all crisis episodes, COVID-19 exerted the strongest impact on South Africa's stock market, exceeding the effects observed during the Global Financial Crisis and the Eurozone debt crisis. Contrary to common expectations, Eurozone markets and Canada exert a stronger influence on the JSE than the United States over extended periods. Japan's NIKKEI 225 consistently emerges as a net receiver of shocks relative to South Africa. Overall, these results confirm that South Africa is structurally embedded within the G7 equity network, with external shocks playing a dominant role in shaping domestic market dynamics.

The bivariate wavelet analysis highlights pronounced heterogeneity in South Africa's co-movement with individual G7 markets across time and frequencies. Strong medium- to long-term integration is observed between the JSE and the S&P 500, with the U.S. market leading South Africa, particularly at horizons between 16 and 64 days. Similar lead–lag patterns are evident for the FTALLSH and DAX during 2006–2010, especially at medium- and long-term scales, though integration weakens in later years. The CAC40 and MIB display semi-strong integration with the JSE during crisis periods, again with leadership originating from European markets. By contrast, the NIKKEI 225 exhibits weak and sporadic integration, with only limited long-horizon influence during major crises. These findings suggest that South Africa's vulnerability to external shocks is driven primarily by U.S. and European equity markets, particularly over medium-term horizons.

The multivariate wavelet results reveal persistently high dependence across all seven investment horizons. WMC values remain between approximately 0.966 and 0.978, indicating strong system-wide co-movement with only modest variation across scales. CAC40 is the maximizing market at every WMC detail level. The WMCC results reinforce this pattern, identifying CAC40 as the maximizing market across all seven scales. The maximum occurs contemporaneously at D_1–D_5 and D_7, while at D_6, corresponding to 64–128 trading days, CAC40 leads the linear combination of the remaining markets by approximately one trading day. These findings indicate strong multivariate dependence and limited evidence of persistent temporal leadership outside the D_6 horizon. They should not be interpreted as evidence of structurally identified causal transmission from France to South Africa, since common euro-area, currency and global financial factors may also contribute to the prominence of CAC40.

The findings have important implications for policymakers and market participants. Policymakers should strengthen macroprudential frameworks and capital-flow monitoring during periods of heightened global stress. For investors, strong multivariate co-movement suggests that diversification benefits between South African and G7 equities may be limited, particularly at medium and long horizons. However, the analysis does not estimate optimal portfolio allocations or realised diversification gains.

Several limitations should be noted. The connectedness measures capture statistical dependence rather than structurally identified causal transmission and may partly reflect common global, monetary, and currency factors. The use of U.S.-dollar-denominated indices may also introduce common currency effects, while crisis comparisons remain descriptive because no formal structural-break tests are conducted. Future research could examine local-currency returns, common-factor controls, formal crisis windows, and broader asset-class or sectoral networks.

References

Agyei-Ampomah, S. (2011). Stock market integration in Africa. *Managerial Finance*, 37(3), 242–256.

Antonakakis, N., Chatziantoniou, I., and Gabauer, D. (2020). Refined measures of dynamic connectedness based on time-varying parameter vector autoregressions. *Journal of Risk and Financial Management*, 13(4), 84.

Batondo, M. and Uwilingiye, J. (2022). Comovement across BRICS and the US stock markets: A multitime scale wavelet analysis. *International Journal of Financial Studies*, 10(2), 27.

Boako, G. and Alagidede, P. (2016). Global commodities and African stocks: A 'market of one'?. *International Review of Financial Analysis*, 44, 226–237.

Bonga-Bonga, L. and Phume, M. P. (2022). Return and volatility spillovers between South African and Nigerian equity markets. *African Journal of Economic and Management Studies*, 13(2), 205–218.

Carmona, R., Hwang, W.-L., and Torresani, B. (1998). *Practical Time-Frequency Analysis: Gabor and wavelet transforms, with an implementation in S*. Academic Press.

Chatziantoniou, I. and Gabauer, D. (2021). EMU risk-synchronisation and financial fragility through the prism of dynamic connectedness. *The Quarterly Review of Economics and Finance*, 79, 1–14.

Cornish, C. R., Bretherton, C. S., and Percival, D. B. (2006). Maximal overlap wavelet statistical analysis with application to atmospheric turbulence. *Boundary-Layer Meteorology*, 119, 339–374.

Diebold, F. X. and Yilmaz, K. (2012). Better to give than to receive: Predictive directional measurement of volatility spillovers. *International Journal of Forecasting*, 28(1), 57–66.

Fernández-Macho, J. (2012). Wavelet multiple correlation and cross-correlation: A multiscale analysis of eurozone stock markets. *Physica A: Statistical Mechanics and its Applications*, 391(4), 1097–1104.

Fisher, R. A. (1915). Frequency distribution of the values of the correlation coefficient in samples from an indefinitely large population. *Biometrika*, 10(4), 507–521.

Gençay, R., Selçuk, F., and Whitcher, B. J. (2001). *An Introduction to Wavelets and Other Filtering Methods in Finance and Economics*. Elsevier.

Gopane, T. J. (2023). Economic integration and stock market linkages: evidence from South Africa and BRIC. *Journal of Economics, Finance and Administrative Science*.

Grinsted, A., Moore, J. C., and Jevrejeva, S. (2004). Application of the cross wavelet transform and wavelet coherence to geophysical time series. *Nonlinear Processes in Geophysics*, 11(5/6), 561–566.

Grossmann, A. and Morlet, J. (1984). Decomposition of hardy functions into square integrable wavelets of constant shape. *SIAM Journal on Mathematical Analysis*, 15(4), 723–736.

Hasan, M. B., Mahi, M., Hassan, M. K., and Bhuiyan, A. B. (2021). Impact of COVID-19 pandemic on stock markets: Conventional vs. Islamic indices using wavelet-based multi-timescales analysis. *The North American Journal of Economics and Finance*, 58, 101504.

In, F. and Kim, S. (2013). *An Introduction to Wavelet Theory in Finance: A wavelet multiscale approach*. World Scientific.

Izzeldin, M., Muradoğlu, Y. G., Pappas, V., and Sivaprasad, S. (2021). The impact of COVID-19 on G7 stock markets volatility: Evidence from a ST-HAR model. *International Review of Financial Analysis*, 74, 101671.

Junior, P. O., Tetteh, J. E., Nkrumah-Boadu, B., and Adjei, A. N. (2024). Comovement of African stock markets: Any influence from the COVID-19 pandemic?. *Heliyon*, 10(9).

Koop, G., Pesaran, M. H., and Potter, S. M. (1996). Impulse response analysis in nonlinear multivariate models. *Journal of Econometrics*, 74(1), 119–147.

Lawrence, B., Obalade, A. A., and Doorasamy, M. (2024a). Interlinkage of Johannesburg stock exchange super sectors during extreme market events. *African Journal of Business and Economic Research*, 19(1), 101–121.

Lawrence, B., Obalade, A. A., Tita, A. F., and French, J. J. (2024b). Stock market connectedness during an energy crisis: Evidence from South Africa. *Emerging Markets Review*, 63, 101194.

Madaleno, M. and Pinho, C. (2012). International stock market indices comovements: a new look. *International Journal of Finance & Economics*, 17(1), 89–102.

Martens, M. and Poon, S.-H. (2001). Returns synchronization and daily correlation dynamics between international stock markets. *Journal of Banking & Finance*, 25(10), 1805–1827.

Mensah, J. O. and Alagidede, P. (2017). How are Africa's emerging stock markets related to advanced markets? Evidence from copulas. *Economic Modelling*, 60, 1–10.

Morlet, J., Arens, G., Fourgeau, E., and Glard, D. (1982). Wave propagation and sampling theory—Part I: Complex signal and scattering in multilayered media. *Geophysics*, 47(2), 203–221.

Nason, G. P. (2008). *Wavelet Methods in Statistics with R*. Springer.

Nyakurukwa, K. and Seetharam, Y. (2022). Stock market integration in Africa: Further evidence from an information-theoretic framework. *International Finance*.

Percival, D. P. (1995). On estimation of the wavelet variance. *Biometrika*, 82(3), 619–631.

Percival, D. B. and Mofjeld, H. O. (1997). Analysis of subtidal coastal sea level fluctuations using wavelets. *Journal of the American Statistical Association*, 92(439), 868–880.

Percival, D. B. and Walden, A. T. (2000). *Wavelet Methods for Time Series Analysis*, volume 4. Cambridge University Press.

Pesaran, H. H. and Shin, Y. (1998). Generalized impulse response analysis in linear multivariate models. *Economics Letters*, 58(1), 17–29.

Pukthuanthong, K. and Roll, R. (2009). Global market integration: An alternative measure and its application. *Journal of Financial Economics*, 94(2), 214–232.

Ramsey, J. B. (2002). Wavelets in economics and finance: Past and future. *NYU Working Paper No. S-MF-02-02*.

Rehman, M. U., Kang, S. H., Ahmad, N., and Vo, X. V. (2021). The impact of COVID-19 on the G7 stock markets: A time-frequency analysis. *The North American Journal of Economics and Finance*, 58, 101526.

Rigobon, R. (2019). Contagion, spillover, and interdependence. *Economía*, 19(2), 69–100.

Roesch, A. and Schmidbauer, H. (2014). *WaveletComp: Computational Wavelet Analysis*. R package.

Statista (2024). Volume of global equity trading. Accessed: 16-Feb-2025.

Tabash, M. I., Chalissery, N., Nishad, T. M., and Al-Absy, M. S. M. (2024). Market shocks and stock volatility: Evidence from emerging and developed markets. *International Journal of Financial Studies*, 12(1), 2.

Tiwari, A. K., Dar, A. B., Bhanja, N., and Shah, A. (2013). Stock market integration in Asian countries: Evidence from wavelet multiple correlations. *Journal of Economic Integration*, 28(3), 441–456.

Torrence, C. and Compo, G. P. (1998). A practical guide to wavelet analysis. *Bulletin of the American Meteorological Society*, 79(1), 61–78.

Torrence, C. and Webster, P. J. (1999). Interdecadal changes in the ENSO–monsoon system. *Journal of Climate*, 12(8), 2679–2690.

Veleda, D., Montagne, R., and Araujo, M. (2012). Cross-wavelet bias corrected by normalizing scales. *Journal of Atmospheric and Oceanic Technology*, 29(9), 1401–1408.

Yaya, O., Adenikinju, O., and Olayinka, H. A. (2024). African stock markets' connectedness: Quantile VAR approach. *Modern Finance*, 2(1).